

Dispersive analysis of low energy pion photo- and electroproduction

Xionghui Cao

In collaboration with Yao Ma and Hanqing Zheng

Peking University

November 17, 2021

Talk given at the 10th International Workshop on Chiral Dynamics
IHEP, Beijing (online)

Contexts

- 1 Background
- 2 Omnès formalism and dispersive representation
- 3 Numerical Analysis
- 4 Electromagnetic couplings of the subthreshold resonance
- 5 Summary

Theoretical studies on π photo- and electroproduction

- ▶ In 1957, CGLN decomposition was established to study π production by using fixed-t DR [Chew et al., 1957];
- ▶ Current algebra results [Gaffney, 1967; Bhatia and Narayanaswamy, 1968];
- ▶ Effective Lagrangian description [Peccei, 1969];
- ▶ Phenomenological models: unitarity isobar model [Drechsel et al., 1999], dynamic model [Kamalov et al., 2001] and JBW model [Mai et al., 2021], et. al.
- ▶ χ PT: one-loop calculations \implies HB χ PT [Bernard et al., 1994], EOMS [Hilt et al., 2013; Guerrero et al., 2019; Guerrero and Vicente, 2020];
- ▶ Unitarity+ χ PT: couple channel N/D description of πN and γN scatterings [Gasparyan and Lutz, 2010], et. al.
See also slides by Ulf-G. Meissner.

Method

- Inhomogeneous Omnès formalism:
 - ▶ Left-hand cut (LHC) contributions $\Leftarrow \chi\text{PT}$;
 - ▶ Right-hand cut (RHC) contributions \Leftarrow Omnès solution.
- Omnès like formalisms have been successfully applied to many other processes:
 - ▶ $\gamma\gamma \rightarrow \pi\pi$ [Mao et al., 2009; Garcia-Martin and Moussallam, 2010; Dai and Pennington, 2014];
 - ▶ $\eta \rightarrow 3\pi$ [Albaladejo and Moussallam, 2017; Colangelo et al., 2018];
 - ▶ Heavy meson decay[Albaladejo et al., 2017; Yao et al., 2018];
 - ▶ π form factors[Ropertz et al., 2018];
 - ▶ XYZ states[Chen et al., 2019];
 - ▶ ...

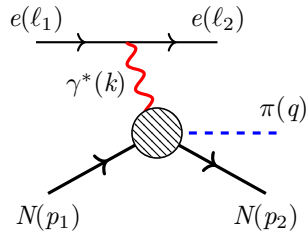
Amplitude decomposition

- Electroproduction: $e(\ell_1) + N(p_1) \rightarrow e(\ell_2) + N(p_2) + \pi(q)$
 $\xrightarrow[\text{approximation}]{\text{OPE}} \gamma^*(k) + N(p_1) \rightarrow N(p_2) + \pi(q) \quad Q^2 = -k^2$

- Lorentz decomposition: $\mathcal{M} = \epsilon_\mu \mathcal{M}^\mu$ [Bernard et al., 1994],

$$\mathcal{M}^\mu = -ie \langle N\pi | J^\mu(0) | N \rangle = \bar{u}(p_2) \left(\sum_{i=1}^6 A_i M_i^\mu \right) u(p_1).$$

ϵ_μ : polarization vector of photon (photoproduction)
or $e \frac{\bar{u}(\ell_1) \gamma_\mu u(\ell_2)}{k^2}$ (electroproduction).



- Isospin decomposition:

$$\mathcal{M}(\gamma^* + N \rightarrow \pi^a + N) = \chi_2^\dagger \left\{ \delta^{a3} \mathcal{M}^{(+)} + i\epsilon^{a3b} \tau^b \mathcal{M}^{(-)} + \tau^a \mathcal{M}^{(0)} \right\} \chi_1,$$

$$\mathcal{M}^{\frac{1}{2}, \frac{1}{2}} = -\sqrt{\frac{1}{3}} (\mathcal{M}^{(+)} + 2\mathcal{M}^{(-)} + 3\mathcal{M}^{(0)}) , \quad \mathcal{M}^{\frac{1}{2}, -\frac{1}{2}} = \sqrt{\frac{1}{3}} (\mathcal{M}^{(+)} + 2\mathcal{M}^{(-)} - 3\mathcal{M}^{(0)}) .$$

CGLN decomposition and PWA

- CGLN amplitude \rightleftharpoons Helicity amplitude
- CGLN decomposition [Chew et al., 1957]: $\mathcal{M}^\mu = \frac{4\pi\sqrt{s}}{m_N} \chi_2^\dagger \mathbf{F} \chi_1$,

$$\begin{aligned}\mathbf{F} = & i\boldsymbol{\sigma} \cdot \mathbf{b} \mathcal{F}_1 + \boldsymbol{\sigma} \cdot \hat{\mathbf{q}} \boldsymbol{\sigma} \cdot (\hat{\mathbf{k}} \times \mathbf{b}) \mathcal{F}_2 + i\boldsymbol{\sigma} \cdot \hat{\mathbf{k}} \hat{\mathbf{q}} \cdot \mathbf{b} \mathcal{F}_3 + i\boldsymbol{\sigma} \cdot \hat{\mathbf{q}} \hat{\mathbf{q}} \cdot \mathbf{b} \mathcal{F}_4 \\ & - i\boldsymbol{\sigma} \cdot \hat{\mathbf{q}} b_0 \mathcal{F}_7 - i\boldsymbol{\sigma} \cdot \hat{\mathbf{k}} b_0 \mathcal{F}_8 \quad (b_\mu = \epsilon_\mu - \frac{\boldsymbol{\epsilon} \cdot \hat{\mathbf{k}}}{|\mathbf{k}|} k_\mu).\end{aligned}$$

- CGLN amplitudes $\xrightarrow[\text{expansion}]{\text{PW}} \mathcal{E}_{l\pm}, \mathcal{M}_{l\pm}, \mathcal{S}_{l\pm}$ [Berends et al., 1967],

$$\mathbb{F}(s, t) = \sum_l \left[\begin{array}{cc} \mathbb{G}_l(x)_{4 \times 4} & \mathbb{O} \\ \mathbb{O} & \mathbb{H}_l(x)_{2 \times 2} \end{array} \right] \mathbb{M}_l(s) \quad (x = \hat{\mathbf{q}} \cdot \hat{\mathbf{k}}),$$

$\mathbb{G}_l(x), \mathbb{H}_l(x)$ both are linear combination of legendre function $P_l(x)$ and its derivative.

Chiral perturbation theory

- Lorentz-invariant chiral Lagrangian up to $\mathcal{O}(p^2)$ [Fettes et al., 2000]:

$$\mathcal{L}_{\text{eff}} = \mathcal{L}_{\pi\pi}^{(2)} + \sum_{i=1}^2 \mathcal{L}_{\pi N}^{(i)},$$

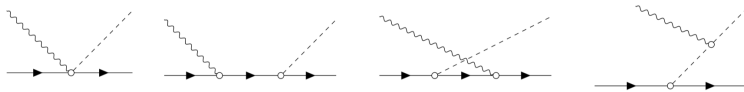
$$\mathcal{L}_{\pi\pi}^{(2)} = \frac{F^2}{4} \text{Tr} \left[D_\mu U (D^\mu U)^\dagger \right] + \frac{F^2}{4} \text{Tr} (\chi U^\dagger + U \chi^\dagger),$$

$$\mathcal{L}_{\pi N}^{(1)} + \mathcal{L}_{\pi N}^{(2)} = \bar{\Psi} \left(i \not{D} - m_N + \frac{g_A}{2} \not{\epsilon} \gamma_5 \right) \Psi + \bar{\Psi} \sigma^{\mu\nu} \left[\frac{c_6}{2} f_{\mu\nu}^+ + \frac{c_7}{2} v_{\mu\nu}^{(s)} \right] \Psi + \dots,$$

pion's parameterization:

$$U(x) = \exp \left(i \frac{\Phi}{F} \right), \quad \Phi = \begin{pmatrix} \pi^0 & \sqrt{2}\pi^+ \\ \sqrt{2}\pi^- & -\pi^0 \end{pmatrix}.$$

- Tree level diagrams[Guerrero et al., 2019]:



Dispersive representation

- PW optical theorem($\mathcal{S} = 1 + 2i\rho\mathcal{T}$):

$$\text{Im } \mathcal{M}(s + i\epsilon) = \mathcal{T}^*(s + i\epsilon)\rho(s + i\epsilon)\mathcal{M}(s + i\epsilon);$$

\implies Unitarity relation: $\mathcal{M}^+ = \mathcal{S}^+\mathcal{M}^-$; ($\mathcal{M}^\pm(s) = \lim_{\epsilon \rightarrow 0} \mathcal{M}(s \pm i\epsilon)$)

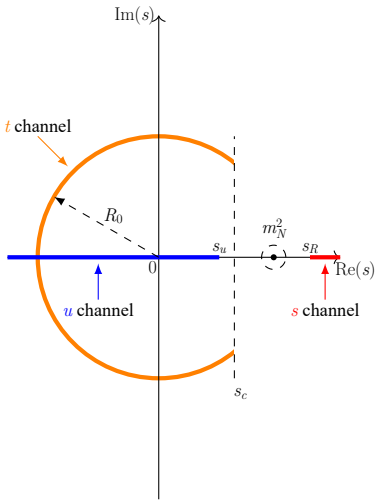
- If the PWA can be divided into two parts: $\mathcal{M} = \mathcal{M}_R + \mathcal{M}_L$;
- Define an auxiliary function, $\Omega(s)$, that only contains RHC and manifests the same unitarity relation as $\mathcal{M}(s)$: $\Omega^+ = \mathcal{S}^+\Omega^-$;
 $\implies \text{Im } (\Omega^{-1}\mathcal{M}_R) = -(\text{Im } \Omega^{-1}) \mathcal{M}_L$;
- ★ n -th subtracted DR for $\text{Im } (\Omega^{-1}\mathcal{M}_R)$ [Babelon et al., 1976]:

$$\boxed{\mathcal{M}^I(s) = \mathcal{M}_L^I(s) + \Omega^I(s) \left(\frac{s^n}{\pi} \int_{s_R}^{\infty} \frac{\sin \delta^I(s') \mathcal{M}_L^I(s')}{|\Omega(s')| s'^n (s' - s)} ds' + \mathcal{P}_{n-1}^I(s) \right)}.$$

Omnès solution [Omnès, 1958]: $\Omega^I(s) = \mathcal{P}^I(s) \exp \left[\frac{s}{\pi} \int_{s_R}^{\infty} \frac{\delta^I(s')}{s'(s'-s)} ds' \right]$.

Singularity structure of PWA ($Q^2 = 0$) [Kennedy and Spearman, 1962]

- I Unitarity cut, $s \in [s_R, \infty)$ on account of s -channel continuous spectrum;
- II t -channel cut, 1. arc stems from $4m_\pi^2 \leq t \leq 4m_N^2$; 2. $s \in (-\infty, 0]$ corresponding to $t \geq 4m_N^2$;
- III u -channel cut,
$$s \in \left(-\infty, s_u = \frac{m_N(m_N^2 - m_\pi^2 - m_\pi m_N)}{m_\pi + m_N} \right] \text{ due to}$$
$$u \geq (m_\pi + m_N)^2;$$
- IV Pole, $s = m_N^2$, due to t -channel pion exchange and u -channel nucleon exchange.



Singularity structure of PWA ($Q^2 \neq 0$)

I Unitarity cut, $s \in [s_R, \infty)$ on account of s -channel continuous spectrum;

II t -channel cut, 1. arc stems from $4m_\pi^2 \leq t \leq 4m_N^2$; 2. $s \in (-\infty, 0]$ corresponding to $t \geq 4m_N^2$;

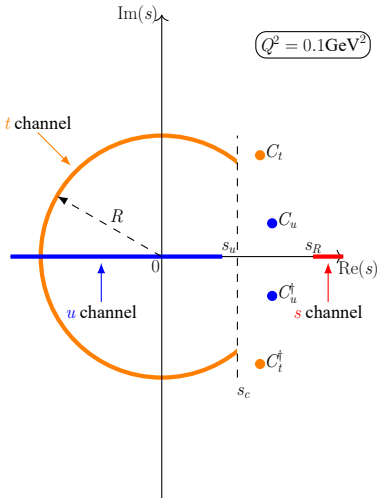
III u -channel cut,

$$s \in \left(-\infty, s_u = \frac{m_N^3 - m_\pi^2 m_N - m_\pi(m_N^2 + Q^2)}{m_\pi + m_N} \right)$$

due to $u \geq (m_\pi + m_N)^2$;

IV Cut due to t -channel pion exchange, the branch points locate at $0, C_t, C_t^\dagger$;

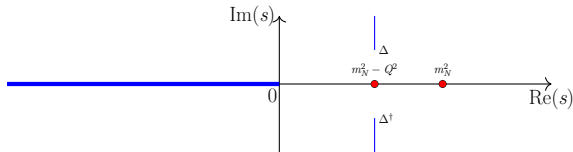
V Cut due to u -channel nucleon exchange, the branch points locate at $0, C_u, C_u^\dagger$.



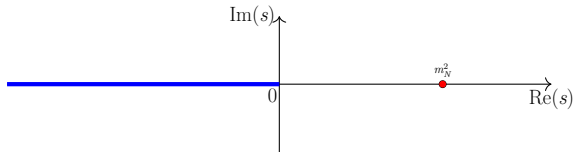
★ In real photon point, $C_t, C_u \xrightarrow{Q^2 \rightarrow 0} m_N^2$

Kinematic singularities

- Kinematic singularities: in our consideration, stems from relativistic kinematics such that $\sqrt{s - s_L} \sqrt{s - s_R}$, etc.



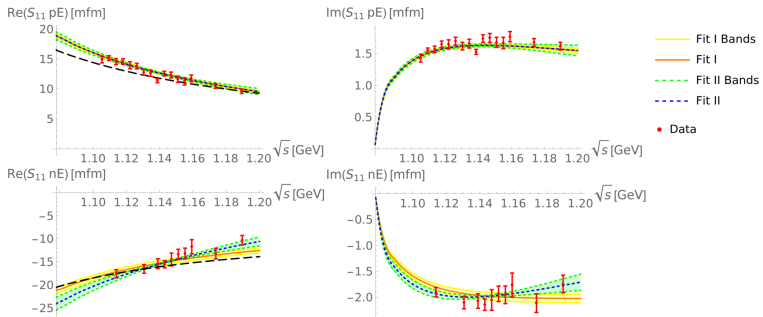
$$\Downarrow (Q^2 \rightarrow 0)$$



- All cuts do not cover the unitarity cut, so the whole singularities can be divided into RHC and LHC.

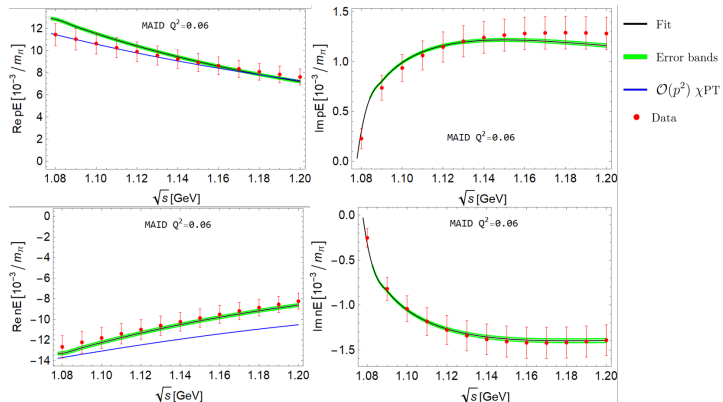
Fit results of photoproduction [Ma et al., 2021]

- Data:
 - ▶ SAID[Workman et al., 2012] \Rightarrow photoproduction;
 - ▶ DMT2001[Kamalov and Yang, 1999] and MAID2007[Drechsel et al., 2007] \Rightarrow electroproduction.
- Fitting S_{11} PW $\rightarrow E_{0+}, S_{0+}$, with p and n targets;
Combination fit: $Q^2 \sim 0 - 0.1\text{GeV}^2$ & $\sqrt{s} \sim 1.08 - 1.2\text{GeV}$;
Phase shifts \Leftarrow Roy-Steiner equation[Hofrichter et al., 2016].



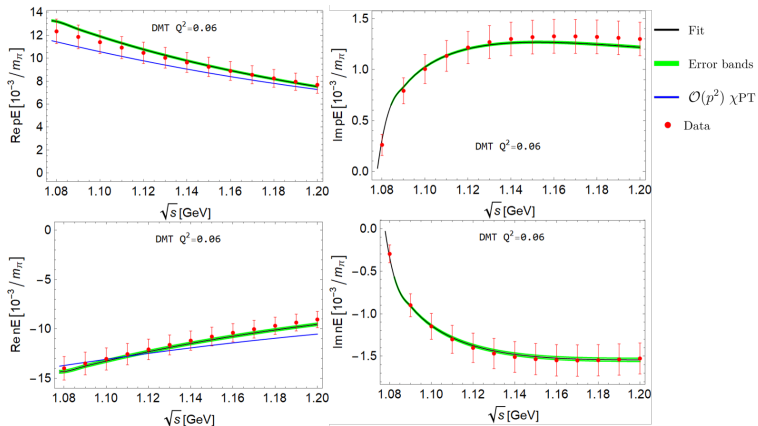
Fit results of electroproduction [Cao et al., 2021] — E_{0+}

- E_{0+} ($Q^2 = 0.06 \text{ GeV}^2$)
- Subtraction constant: independent of Q^2 when neglecting the contribution of vector meson.



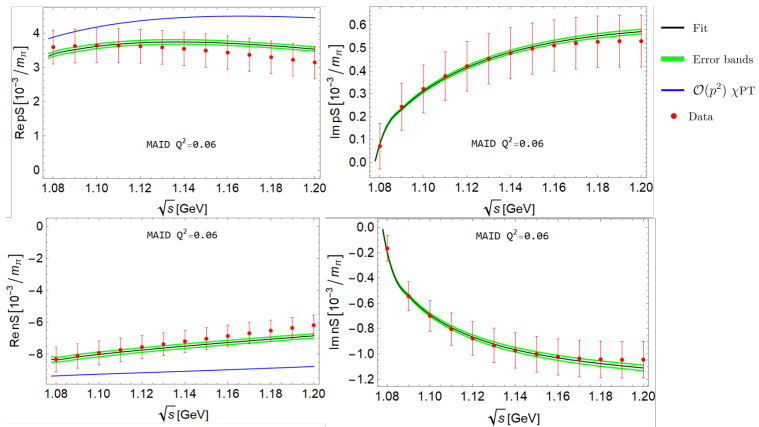
Fit results of electroproduction— E_{0+}

- E_{0+} ($Q^2 = 0.06 \text{ GeV}^2$)



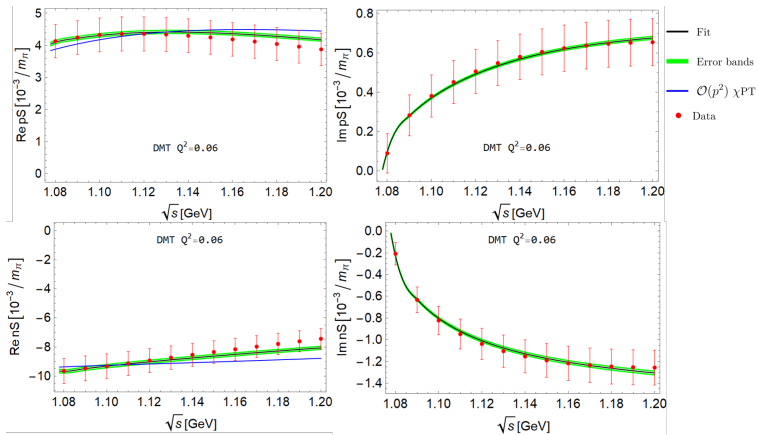
Fit results of electroproduction— S_{0+}

- S_{0+} ($Q^2 = 0.06 \text{ GeV}^2$)



Fit results of electroproduction— S_{0+}

- S_{0+} ($Q^2 = 0.06 \text{ GeV}^2$)



Fit discussion

- ▶ Estimating error bars according to $\text{err}(\mathcal{M}) = \sqrt{(e_s)^2 + (e_r)^2 (\mathcal{M})^2}$,
 $e_s^{R,I} = 0.4, 0.1 [10^{-3}/m_\pi]$, $e_r = 10\%$;
- ▶ Truncation of the DR: Λ dependence \rightleftharpoons subtraction constant a ;

$$\frac{s}{\pi} \int_{s_R}^{\Lambda} \frac{\sin \delta^I(s') \mathcal{M}_L^I(s')}{|\Omega(s')| s' (s' - s)} ds' + a$$

- ▶ $\mathcal{O}(p^4)$ [Hilt et al., 2013], $\mathcal{O}(p^3)$ with Δ [Guerrero et al., 2019; Guerrero and Vicente, 2020] calculations are advantageous compared with an $\mathcal{O}(p^2)$ calculation;
- ▶ Unitarization effects are automatically fulfilled in our scheme.

Analytic continuation

- ▶ Possible hidden pole $N^*(890)$ in S_{11} channel [Wang et al., 2018; Li et al., 2021].
- ▶ Pion photo- and electroproduction \rightarrow Electromagnetic couplings
- ▶ Analytical continuation to second sheet:

$$\mathcal{M}^{\text{II}}(s) = \frac{\mathcal{M}(s)}{\mathcal{S}(s)} \xrightarrow{\mathcal{S}(s) \simeq \mathcal{S}'(s_p)(s - s_p)} \mathcal{M}^{\text{II}}(s) \simeq \frac{\mathcal{M}(s)}{\mathcal{S}'(s_p)(s - s_p)}.$$

- ▶ The couplings are defined as the residue via:

$$\mathcal{M}^{\text{II}}(s \rightarrow s_p) \simeq \frac{g_{\gamma N} g_{\pi N}}{s - s_p}, \quad \mathcal{T}^{\text{II}}(s \rightarrow s_p) \simeq \frac{g_{\pi N}^2}{s - s_p},$$

$$\Rightarrow \boxed{g_{\gamma N} g_{\pi N} \simeq \frac{\mathcal{M}(s_p)}{\mathcal{S}'(s_p)}, \quad g_{\pi N}^2 \simeq \frac{\mathcal{T}(s_p)}{\mathcal{S}'(s_p)}}.$$

Residues photon decay amplitudes

- Residue \Rightarrow Decay amplitude [Workman et al., 2013a; Tiator et al., 2016]

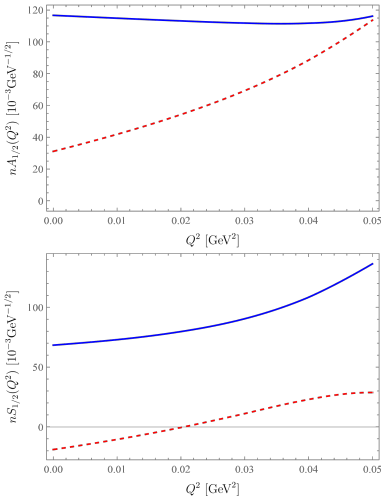
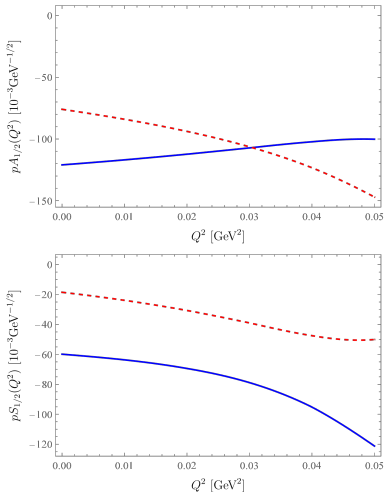
$$A_{1/2}^{\text{pole}}(Q^2) = g_{\gamma N}^E \sqrt{\frac{3\pi W_p}{m_N k_p^{\text{cm}}}}, \quad S_{1/2}^{\text{pole}}(Q^2) = g_{\gamma N}^S \sqrt{\frac{3\pi W_p}{2m_N k_p^{\text{cm}}}}$$

Target	Pole Position	$g_{\pi N} \cdot g_{\gamma N}(10^{-2} \text{GeV}^2)$		$A_{1/2}(\text{GeV}^{-1/2})$	
		Moduli	Phase (degree)	Moduli	Phase (degree)
p	$0.882 + 0.190i$	1.212	-79	0.17	-129
	$0.960 + 0.192i$	1.467	-71	0.19	-43
n	$0.882 + 0.190i$	0.642	111	0.09	62
	$0.960 + 0.192i$	1.111	103	0.14	130

- $N^*(890)$ vs $N^*(1535)$:

	$N^*(890)$	$N^*(1535)$
$ g_{\pi N} ^2$	0.2 GeV ² [Wang et al., 2018]	0.08 GeV ² [Arndt et al., 2006]
$ g_{\gamma N} $	0.032 GeV [Ma et al., 2021]	0.024 GeV [Workman et al., 2013b; Švarc et al., 2014]
$ p A_{1/2} $	0.17 GeV ^{-1/2} [Ma et al., 2021]	0.007 GeV ^{-1/2} [Workman et al., 2013b; Švarc et al., 2014]

Virtual-photon decay amplitudes



Pole position: $\sqrt{s} = 0.89 - 0.19i$ in the unit of GeV.

Summary

- I Single pion photo- and electroproduction are analyzed at low energies using a dispersive representation;
- II The analytic structure of PWA;
- III χ PT+Omnès solution with a few parameters \implies describing data at $Q^2 \leq 0.1 \text{ GeV}^2$;
- IV The residues $|g_{\pi N}|$ of $N^*(890)$ is large than $N^*(1535)$. However, $|g_{\gamma N}|$ is comparable with $N^*(1535)$.

Thanks for Listening!